

Structure and Bonding in the Omnicapped Truncated Tetrahedral Au₂₀ Cluster: Analogies between Gold and Carbon Cluster Chemistry

R. Bruce King,* Zhongfang Chen, and Paul von Ragué Schleyer

Department of Chemistry, University of Georgia, Athens, Georgia 30602

Received March 19, 2004

The proposed omnicapped truncated tetrahedral structure of the recently reported Au₂₀ cluster can be generated from a regular dodecahedron by forming two transannular Au–Au bonds across each face while preserving *T* symmetry. An electron-precise chemical bonding scheme accounts for the large band gap (1.77 eV) of Au₂₀ and relates its structure to that of titanacarbohedrene Ti₈C₁₂ and Os₂₀(CO)₄₀²⁻.

The remarkable recent discovery of the Au₂₀¹ gold cluster, generated by the laser vaporization of a pure gold target with a helium carrier gas, has analogies with the well-known preparation of C₆₀.² The large band gap of Au₂₀ (1.77 eV from the PE spectrum) is about 0.2 eV greater than that of C₆₀. Relativistic DFT calculations favor an Au₂₀¹ structure based on an omnicapped truncated tetrahedron (Figure 1, a “ ν_3 -tetrahedron”).³ We now extend ideas from previous studies on gold clusters^{4–6} to describe the bonding in Au₂₀. In addition, Au₂₀ is compared with other related M₂₀ cluster polyhedra, the “metcar” Ti₈C₁₂ and the metal carbonyl anion⁷ Os₂₀(CO)₄₀²⁻.

The ν_3 -tetrahedral structure for Au₂₀ can be derived from a regular dodecahedron by adding two transannular Au–Au bonds across each of the 12 pentagonal faces in such a way that tetrahedral rotational symmetry (*T*) is preserved. Figure 2 shows one of the resulting four macrotriangular faces of the ν_3 -tetrahedron with the edges of the original pentagonal dodecahedral faces of the regular dodecahedron in black and the new transannular interactions in red. The original 30 edges of the regular dodecahedron are thus supplemented by 12 × 2 = 24 new edges leading to the 54

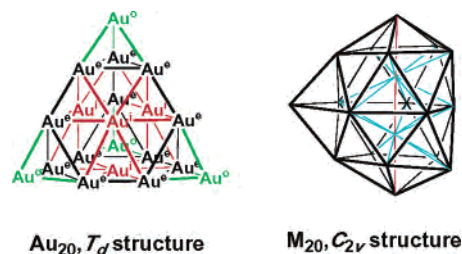


Figure 1. The two 20-vertex polyhedra considered for M₂₀ clusters. See text for color codes and explanation.



Figure 2. A triangular face of the ν_3 -tetrahedron proposed for Au₂₀ showing the internal bonds on the original pentagonal dodecahedron face in black and the new bonds in red.

edges required by Euler’s theorem⁸ for a 20-vertex deltahedron. In addition, the four gold atoms in the center of the four macrotriangular faces (Auⁱ in Figure 1) form a central Au₄ tetrahedral cavity with six additional “internal” edges corresponding to additional Au–Au interactions.

The gold atoms in the resulting structure are divided into three types in Figure 1 (left side), namely, the four outer capping Au^o atoms (green), 12 edge Au^e atoms (black), and four inner Auⁱ atoms (red). If each of these 20 gold atoms retains its filled d¹⁰ shell, then each contributes a single electron for the skeletal bonding. The resulting 20 electrons can be used to form a four-center two-electron (4c–2e) bond in each of 10 tetrahedral cavities of the following two types: (1) four Au^oAu^e₃ tetrahedral cavities at the outer four vertices of the ν_3 -tetrahedron; (2) six Au^e₂Auⁱ₂ tetrahedral cavities in the middle of the six edges of the ν_3 -tetrahedron. This chemical bonding model has the advantage that the filled d¹⁰ shells of all three types of gold atoms remain intact.

Figure 3 compares related carbon and gold structures showing the generation of new metal–metal bonds in the gold clusters. As shown, the three-dimensional ν_3 -macrotetrahedral structure proposed for Au₂₀ bears a relationship to the regular dodecahedral structure of C₂₀ similar to the relationship that benzene bears to the two-dimensional σ -aromatic macrotriangular structure calculated⁹ for the experimentally observed Au₅Zn⁺. In both cases relatively sym-

* Author to whom correspondence should be addressed. E-mail: rbking@sunchem.chem.uga.edu.

- (1) Li, J.; Li, X.; Zhai, H.-J.; Wang, L. S. *Science* **2003**, *299*, 864.
- (2) Kroto, H. W.; Allaf, A. W.; Balm, S. P. *Chem. Rev.* **1991**, *91*, 1212.
- (3) For this nomenclature see: Teo, B. K.; Sloane, N. J. A. *Inorg. Chem.* **1986**, *25*, 2315. ν_3 designates the three connections at each tetrahedral edge.
- (4) King, R. B. *Inorg. Chim. Acta* **1986**, *116*, 109.
- (5) King, R. B. *J. Chem. Inf. Comput. Sci.* **1994**, *34*, 410.
- (6) King, R. B. *Inorg. Chim. Acta* **1998**, *277*, 202.
- (7) Gade, L. H.; Johnson, B. F. G.; Lewis, J.; McPartlin, M.; H. R. Powell, H. R.; Raithby P. R.; Wong, W.-T. *J. Chem. Soc., Dalton Trans.* **1994**, 521.
- (8) King, R. B. *Applications of Graph Theory and Topology in Inorganic Cluster and Coordination Chemistry*; CRC Press: Boca Raton, 1993; pp 10–12.

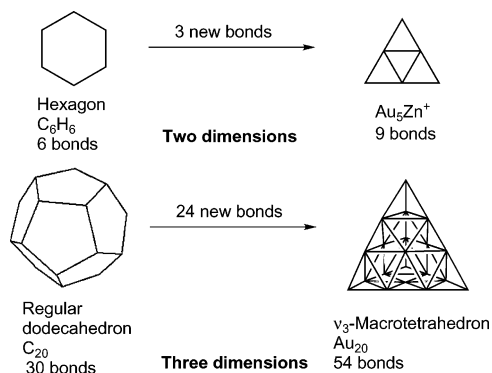


Figure 3. Carbon clusters versus gold clusters: generation of new Au–Au edges through aurophilic interactions.

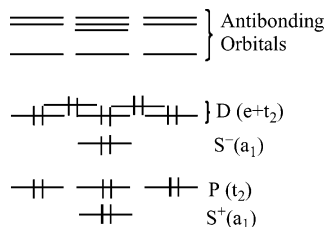


Figure 4. Molecular orbital energy levels in an Au_{20} ν_3 -tetrahedron showing both the spherical harmonic and group-theoretical labels for the bonding orbitals.

metrical networks of M_3 triangles are generated by transannular interactions across a hexagon as in benzene $\rightarrow \text{Au}_5\text{Zn}^+$ or across the 12 pentagonal faces of the dodecahedron as in $\text{C}_{20} \rightarrow \text{Au}_{20}$. The formation of ν_3 -tetrahedral Au_{20} from the hypothetical regular dodecahedral Au_{20} by addition of 24 new transannular bonds (as shown in Figure 2) can be contrasted with the formal trimerization of C_{20} to the stable truncated icosahedral C_{60} fullerene by a “leapfrog” transformation.^{10,11} Thus heavy metals such as gold favor cluster structures based on networks of triangles whereas carbon favors clusters containing pentagons and hexagons. As a result, totally different processes are used to convert the hypothetical pentagonal dodecahedral C_{20} and Au_{20} to stable species.

The B3LYP/Lan12dz geometries and vibrational frequencies of 20-vertex Cu, Ag, Au, K, Rb, and Cs clusters with T_d and C_{2v} symmetries were computed with Gaussian 98.¹² Li_{20} and Na_{20} frequencies are at B3LYP/6-31G* and final geometries at B3LYP/6-311+G*.

Figure 4 plots the energy levels of the 20 molecular orbitals generated by overlap of the intracluster orbitals of the 20 gold atoms in the ν_3 -tetrahedral Au_{20} . The MO pattern of the simplest M_{20} (T_d) is $(a_1)(t_2)^3(a_1)(t_2)^3(e)^2$ (Figure 4). The spherical harmonic pattern^{13–16} of Au_{20} (T_d) is similar to that in other deltahedral clusters exhibiting spherical aromaticity.^{17,18} Nucleus-independent chemical shifts (NICS)¹⁹ were computed to assess the electron delocalization (Table

Table 1. Relative Energies Computed for the T_d , C_{2v} , and C_s Structures of M_{20} Clusters^a

	symmetry	E_{rel} , kcal/mol	NICS(0)	E_{at} , kcal/mol
Cu ₂₀	T_d	0.0	−19.5	920.1
	C_{2v}	3.6	−81.3	916.4
	C_s^b	0.3		920.
	C_1	−0.6		920.5
Ag ₂₀	T_d	0.0	−17.4	671.2
	C_{2v}	27.3	−64.4	643.6
	C_s^b	12.6		658.5
	C_1	12.1		659.0
Au ₂₀	T_d	0.0	−17.7	823.6
	C_s	39.5		783.7
Li ₂₀ ^c	T_d	0.0	7.9	438.1
	C_{2v}	−22.4	−42.4	461.3
Na ₂₀ ^c	T_d	0.0	−12.6	293.2
	C_{2v}	3.3	−46.1	290.4
	C_s	−0.7		294.1
K ₂₀	T_d	0.00	−9.2	213.4
	C_{2v}	4.46	−37.8	208.9
	C_s	0.98		212.4
Rb ₂₀	T_d	0.00	−10.8	173.2
	C_{2v}	8.23	−36.2	164.9
	C_s	2.49		170.8
Cs ₂₀	T_d	0.00	−9.8	149.5
	C_{2v}	7.65	−29.5	141.8
	C_s^d	7.64		141.8
	C_s	2.24		147.3

^a Minima computed at the B3LYP/LanL2DZ level, unless indicated otherwise. ^b $N_{\text{imag}} = 1$, distorted to C_1 symmetry. ^c Data at B3LYP/6-311+G** with B3LYP/6-31G* zero point energy corrections. ^d The Cs_{20} structure has one imaginary frequency, but the true C_s minimum, a distorted pseudo- C_{2v} structure, has essentially the same energy.

1). NICS is a simple and effective aromaticity measure. Negative NICS values characterize the electron delocalization associated with aromaticity.

Similar to C_{60} and other fullerenes,²⁰ Au_{20} (T_d) also has degenerate low-lying LUMO orbitals. The computed energy differences for the (LUMO) – (LUMO + 1), (LUMO + 1) – (LUMO + 2), and (LUMO + 2) – (LUMO + 3) separations are 0.36, 0.01, and 0.05 eV, respectively (the HOMO–LUMO gap is 2.94 eV). Thus, Au_{20} (T_d) is likely to be reducible (to the hexaanion) and may readily react with nucleophiles like fullerenes. In this connection, the experimentally measured larger electron affinity of Au_{20} compared with that of C_{60} already shows that Au_{20} is more electronegative than C_{60} . The natural charges obtained from natural population analysis²¹ for the three types of gold atoms in Au_{20} (T_d) are −0.134 ($\text{Au}^{\delta-}$), 0.023 (Au^{δ}), and 0.064 ($\text{Au}^{\delta+}$), respectively. This suggests that nucleophiles will prefer to attack the gold atoms at the vertices ($\text{Au}^{\delta-}$), while electrophiles will prefer to attack the gold atoms at the edges ($\text{Au}^{\delta+}$) and face midpoints (Au^{δ}) of the ν_3 -tetrahedron. The HOMO and LUMO orbitals presented in Figure 5 lead to the same conclusion for the preferred sites as found above.

Alternative C_{2v} and C_s structures for M_{20} clusters²² consist of an outer 18-vertex deltahedron with two inner vertices

(9) Tanaka, H.; Neukermans, S.; Janssens, E.; Silverans, R. E.; Lievens, P. *J. Am. Chem. Soc.* **2003**, *125*, 2862.
 (10) Fowler, P. W.; Steer, J. I. *J. Chem. Soc., Chem. Commun.* **1987**, 1403.
 (11) Fowler, P. W.; Redmond, *Theor. Chim. Acta* **1992**, *83*, 367.
 (12) Frisch, M. J.; et al. Gaussian 98; Gaussian, Inc.: Pittsburgh, PA, 1998.
 (13) Stone, A. J. *Inorg. Chem.* **1981**, *20*, 563.
 (14) Stone, A. J.; Alderton, J. J. *Inorg. Chem.* **1982**, *21*, 2297.
 (15) Stone, A. J. *Polyhedron* **1984**, *3*, 1299.
 (16) Johnston, R. L.; Mingos, D. M. P. *Theor. Chim. Acta* **1989**, *75*, 11.

(17) Hirsch, A.; Chen, Z.; Jiao, H. *Angew. Chem., Int. Ed.* **2001**, *40*, 2834.
 (18) Bühl, M.; Hirsch, A. *Chem. Rev.* **2001**, *101*, 1153.
 (19) Schleyer, P. v. R.; Maerker, C.; Dransfeld, A.; Jiao, H.; Hommes, N. J. R. v. E. *J. Am. Chem. Soc.* **1996**, *118*, 6317.
 (20) Sternfeld, T.; Thilgen, C.; Chen, Z.; Siefken, S.; Schleyer, P. v. R.; Thiel, W.; Diederich, F.; Rabinovitz, M. *J. Org. Chem.* **2003**, *68*, 4850.
 (21) Reed, A. E.; Weinstock, R. B.; Weinhold, F. *J. Chem. Phys.* **1985**, *83*, 735.
 (22) J. Wang, G. Wang, J. Zhao, *Chem. Phys. Lett.* **2003**, *380*, 716.

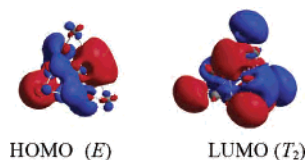


Figure 5. Frontier molecular orbitals of Au_{20} (T_d).

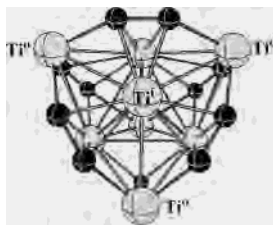


Figure 6. The schematic structure of Ti_8C_{12} (T_d). Representative Ti atoms are labeled.

($\text{M}_2@M_{18}$) (Figure 1, right side) and an outer 19-vertex deltahedron ($M@M_{19}$) with one inner vertex, respectively. Such species also are highly aromatic, since the electron shells of the outer atoms are completely filled, as in In_7O^+ .²³ The C_{2v} structure of Li_{20} is computed have the lowest energy. While Na_{20} was claimed to favor T_d symmetry,²⁴ the C_s isomer is 0.7 kcal/mol more stable. The C_s geometry of Cu_{20} is not a local minimum at B3LYP/LanL2DZ; mode following of its imaginary frequency led to a distorted form, which is -0.6 kcal/mol below the T_d isomer. Other coinage ($M = \text{Ag}, \text{Au}$) and heavier alkali metals ($M = \text{K}, \text{Rb}, \text{Cs}$) prefer T_d to C_{2v} structures energetically (Table 1).

The atomization energies (E_{at}) of the alkali clusters decrease down the periodic table (Table 1). The same trend holds for clusters of the coinage metals copper and silver. However, gold clusters have much larger atomization energy than silver owing to the strong relativistic effects in gold chemistry.²⁵

Although the T_d isomer of Au_{20} is similar to that of the lowest energy structure computed for Ti_8C_{12} (Figure 6),^{26–28} our proposed chemical bonding scheme for Au_{20} , with 10 $4c-2e$ bonds in tetrahedral cavities, is quite different from that suggested²⁹ for T_d Ti_8C_{12} . Analogies with well-established organometallic chemical bonding principles suggest a model for Ti_8C_{12} with 12 Ti^0-C $2c-2e$ σ -bonds and 12 Ti^0C_2 π -bonds to the six alkyne-like C_2 fragments located in the middle of the six edges of the ν_3 -tetrahedron.

The metal carbonyl anion⁷ $\text{Os}_{20}(\text{CO})_{40}^{2-}$ has been found by X-ray diffraction to have an omnicaapped truncated tetrahedral arrangement of metal atoms similar to that computed for Au_{20} and related M_{20} clusters.³⁰ If the carbonyl groups in $\text{Os}_{20}(\text{CO})_{40}^{2-}$ are assumed to be the usual donors of two electrons, then each $\text{Os}(\text{CO})_2$ building block is iso-

electronic with Au^- making $\text{Os}_{20}(\text{CO})_{40}^{2-}$ isoelectronic with Au_{20}^{22-} rather than neutral Au_{20} . As a result, the chemical bonding schemes in $\text{Os}_{20}(\text{CO})_{40}^{2-}$ and Au_{20} must be quite different. The Os_{20} deltahedron (54 edges) + an internal Os_4^i tetrahedron (6 edges) in $\text{Os}_{20}(\text{CO})_{40}^{2-}$ have a total of 60 edges corresponding to an average vertex degree of 6. The 20 $\text{Os}(\text{CO})_2$ units in $\text{Os}_{20}(\text{CO})_{40}^{2-}$ with this average vertex degree of 6 provide an average of 6 skeletal electrons each. This leads to the $20 \times 6 = 120$ skeletal electrons required for two-center two-electron bonds along each of the 60 edges. The remaining two electrons in the $\text{Os}_{20}(\text{CO})_{40}^{2-}$ dianion can possibly form a $4c-2e$ bond in the central tetrahedral cavity similar to the 10 $4c-2e$ bonds postulated above for Au_{20} .

Our chemical bonding analysis and computations indicate that Au_{20} is a stable aromatic gold cluster constructed conceptually from a regular dodecahedron through symmetrical transannular interactions in each of the pentagonal faces (Figure 3). Just like C_{60} , which was isolated in the pure form a few years after its special stability was recognized, it may be possible to isolate Au_{20} as a discrete molecular species. In addition the ν_3 -tetrahedral Au_{20} might serve as a structural unit for new types of stable gold cluster complexes. The negative natural charges (-0.134 e) suggest that the vertex gold atoms (Au^0 in Figure 1) would be possible sites for ligand coordination. Possible synthetic targets of this type might include the following:

(1) Binary gold carbonyls of the types $\text{Au}_{20}(\text{CO})_8$ and $\text{Au}_{20}(\text{CO})_{12}$ having $\text{Au}(\text{CO})_2$ or $\text{Au}(\text{CO})_3$ units at the vertices of the ν_3 -tetrahedron. These species would represent the first known neutral homoleptic gold carbonyls.

(2) The well-known high affinity of gold for sulfur suggests that Au_{20} might form stable complexes with organic sulfides. Reasonable synthetic targets might be complexes of the type $(\eta^2\text{-MeSCH}_2\text{CH}_2\text{SMe})_4\text{Au}_{20}$ with the sulfur ligands coordinated to the vertex gold atoms Au^0 . In this connection recent evidence was obtained for the formation of triphenylphosphine complexes of Au_{20} by a solution synthesis.³¹

In addition, the ν_3 -tetrahedral Au_{20} structure provides a model of a gold surface with three different types of reactive gold sites to bind different molecules for catalysis such as CO , CO_2 , and O_2 . In this connection nucleophilic substrates such as CO might be expected to prefer the Au^0 vertex sites whereas electrophilic substrates such as CO_2 and O_2 might prefer the Au^e edge or Au^i face sites.

Acknowledgment. This work was partially supported by National Science Foundation under Grant CHE-0209857.

Supporting Information Available: Total energies (au), number of imaginary frequencies, zero-point energies (au), and optimized structures of M_{20} clusters. This material is available free of charge via the Internet at <http://pubs.acs.org>.

IC049628R

(23) Janssens, E.; Neukermans, S.; Vanhoutte, F.; Silverans, R. E.; Lievens, P.; Navarro-Vázquez, A.; Schleyer, P. v. R. *J. Chem. Phys.* **2003**, *118*, 5862.

(24) Solov'yov, I. A.; Solov'yov, A. V.; Greiner, W. *Phys. Rev. A* **2002**, *65*, 053203.

(25) Kaltsoyannis, N. *J. Chem. Soc., Dalton Trans.* **1997**, 1.

(26) Dance, I. *J. Am. Chem. Soc.* **1996**, *118*, 2699.

(27) Lin, Z.; Hall, M. B. *J. Am. Chem. Soc.* **1993**, *115*, 11165.

(28) Rohmer, M.-M.; Bénard, M.; Henriot, C.; Bo, C.; Poblet, J. M. *J. Am. Chem. Soc.* **1995**, *117*, 508.

(29) King, R. B. *Inorg. Chem.* **2000**, *39*, 2906.

(30) All of the CO groups in $\text{Os}_{20}(\text{CO})_{40}^{2-}$ are terminal: each of the four pyramid vertex Os atoms is attached to three CO groups; each of the 12 edge Os atoms is attached to two CO groups, and each of the four face-center Os atoms is attached to one CO group.

(31) Zhang, H.-F.; Stender, M.; Zhang, R.; Wang, C.; Li, J.; Wang, L.-S. *J. Phys. Chem. B*, ASAP (Release date May 19, 2004).